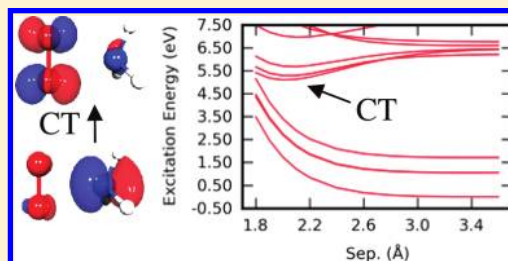


## Computational Investigation of Amine–Oxygen Exciplex Formation

Levi M. Hauptert, Garth J. Simpson, and Lyudmila V. Slipchenko\*

Department of Chemistry, Purdue University, West Lafayette, Indiana 47907, United States

**ABSTRACT:** It has been suggested that fluorescence from amine-containing dendrimer compounds could be the result of a charge transfer between amine groups and molecular oxygen [Chu, C.-C.; Imae, T. *Macromol. Rapid Commun.* **2009**, *30*, 89.]. In this paper we employ equation-of-motion coupled cluster computational methods to study the electronic structure of an ammonia–oxygen model complex to examine this possibility. The results reveal several bound electronic states with charge transfer character with emission energies generally consistent with previous observations. However, further work involving confinement, solvent, and amine structure effects will be necessary for more rigorous examination of the charge transfer fluorescence hypothesis.



## INTRODUCTION

Curious blue-green luminescence has been observed from poly(amidoamine) (PAMAM), poly(propylene imine) (PPI), and poly(ethylene imine) (PEI) dendrimers.<sup>1–3</sup> After discovering increased luminescence from dendrimers containing additional interior tertiary amines, and decreased luminescence from oxygen-deprived samples, Chu and Imae hypothesized that the fluorescence is related to a confined amine–oxygen exciplex charge transfer (CT) transition.<sup>4</sup> To test the hypothesis, Chu and Imae examined the fluorescence properties of triethylamine (TEA) solutions prepared in the absence of oxygen and the same solutions with oxygen-generating dopants introduced. The oxygen-doped TEA solution produced broad-band fluorescence centered at 460 nm with an excitation at 365 nm, similar to the behavior of a fourth generation PAMAM dendrimer.

Little theoretical work has been done with regard to Chu and Imae's hypothesis. Electronic excited states of the NH<sub>3</sub>–O<sub>2</sub> complex were studied using AM1 and PM3 methods by Juranic et al.<sup>5</sup> Both AM1 and PM3 predict a triplet ground state bound by less than 1 kcal mol<sup>–1</sup> with relatively unperturbed ammonia and oxygen geometries and N–O distances between 3 and 4 Å. Relatively low lying triplet states with ~2 Å N–O bond lengths and significant charge transfer character were also predicted. Though the work of Juranic et al. was not originally intended to address the hypothesis of Chu and Imae, it appears to be a logical starting point for ab initio investigations of the hypothesis.

Here we employ ab initio techniques to examine the electronic structure of NH<sub>3</sub>–O<sub>2</sub> in order to build a theoretical model to describe the behavior of charge transfer exciplex states in oxygen–tertiary amine systems.

## THEORY AND METHODOLOGY

Most of the calculations in this work have been performed with the equation-of-motion coupled cluster (EOM-CC) methods.<sup>6–8</sup> In EOM-CC, one finds the electronic excited states by diagonalizing the similarity transformed Hamiltonian  $\bar{H} = e^{-T}He^T$ :

$$\bar{H}R = ER \quad (1)$$

where  $T$  and  $R$  are general excitation operators with respect to the reference state  $|\Phi_0\rangle$ . For example, in the second quantization form

$$\begin{aligned} T &= T_1 + T_2 + \dots \\ &= \sum_{ia} t_i^a a^+ i + \frac{1}{4} \sum_{ijab} t_{ij}^{ab} a^+ b^+ j i + \dots \end{aligned} \quad (2)$$

Here and later,  $i, j$ , etc. denote occupied orbitals in the reference state;  $a, b$ , etc. denote virtual orbitals; and  $t$  are the corresponding single and double amplitudes. The  $t$  amplitudes satisfy the coupled cluster (CC) equations for the reference state:<sup>9</sup>

$$\langle \Phi | \bar{H} | \Phi \rangle = E_{CC} \quad (3)$$

$$\langle \Phi_\mu | \bar{H} | \Phi \rangle = 0 \quad (4)$$

where  $\Phi_\mu$  denotes the  $\mu$ -tuply excited determinants ( $\Phi_i^a, \Phi_{ij}^{ab}$ , etc.) and  $E_{CC}$  is the coupled cluster energy. The eigenstates of  $H$  can be found as

$$|\Psi\rangle = \text{Re}^T |\Phi_0\rangle \quad (5)$$

In practice, both  $R$  and  $T$  operators are truncated; truncation at the level of singles and doubles ( $T = T_1 + T_2$ ;  $R = R_1 + R_2$ ) results in the EOM-CCSD method. EOM-CC(2,3) is defined by truncating  $T$  at the level of singles and doubles and  $R$  at singles, doubles, and triples.<sup>10,11</sup> EOM-CC methods with the same level of truncation in  $T$  and  $R$  are size-extensive. EOM-CC(2,3) is not fully size-extensive; however, the transition energies between different excited states (not including the reference state) are size-extensive.<sup>11</sup>

The choice of the reference state and the  $R$  excitation operator defines a type of EOM-CC. The spin-preserving excitation operator (only  $\alpha \rightarrow \alpha$  and  $\beta \rightarrow \beta$  excitations are included) determines the traditional excitation energy (EE) EOM-EE-CC method.<sup>12,13</sup> In spin-flip (SF) EOM-CC,<sup>14,15</sup> each excitation

Received: June 22, 2011

Published: August 03, 2011

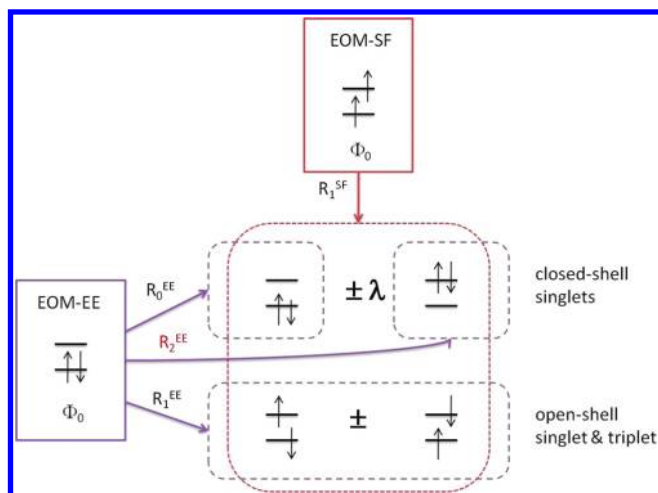


**Figure 1.** Comparison of EOM-EE and EOM-SF for a two-electrons-on-two orbitals system.  $M_s = 0$  determinants are shown. A linear combination of the closed-shell determinants produces two closed-shell singlets. The open-shell determinants combine in an open-shell singlet and a triplet. SF approach describes all these determinants through single excitations ( $R_1^{\text{SF}}$ ) from the high-spin  $M_s = 1$  triplet reference. The excitation energies EE approach provides an unbalanced description of the closed-shell singlets, in which one component is a reference determinant ( $R_0^{\text{EE}}$ ) while the other one is a doubly excited determinant ( $R_2^{\text{EE}}$ ).

involves a spin-flip of one electron, typically,  $\alpha \rightarrow \beta$ . Thus, the SF excitation operator lowers the total spin  $M_s$  of the electronic state. For targeting  $M_s = 0$  electronic states (singlets and triplets), a high spin  $M_s = 1$  reference state is employed in the SF approach:

$$\Psi_{M_s=0}^{s,t} = R_{M_s} = -1 \Psi_{M_s=+1}^t \quad (6)$$

The excitation energy EE variant of EOM-CC is typically used for the description of the electronic states of the closed-shell molecules, as well as Rydberg and mixed valence Rydberg states.<sup>13</sup> The SF variant is a method of choice for targeting diradical states and bond breaking.<sup>13,15–18</sup> A comparison of EE and SF excitations for a system of two electrons on two orbitals is shown in Figure 1.

Other variants of EOM-CC include ionization potential<sup>19–21</sup> (IP) and electron affinity<sup>22</sup> (EA) methods in which the excitation operator annihilates or creates an electron, double IP and double EA (annihilation or creation of two electrons),<sup>23,24</sup> etc. These models are useful for describing radicals and other systems with high degeneracies.

## COMPUTATIONAL DETAILS

The ground state equilibrium geometry of triplet  $\text{NH}_3\text{--O}_2$  was first optimized in the Q-Chem<sup>25</sup> electronic structure package with B3LYP<sup>26–28</sup>/6-31G<sup>\*,29,30</sup> and the resulting structure was refined using EOM-SF-CCSD/6-311+G<sup>\*\*</sup>.<sup>31,32</sup> The geometry optimizations were confined to  $C_s$  symmetry.

Molecular orbitals for the ammonia–oxygen system were computed in GAMESS<sup>33,34</sup> with Hartree–Fock (HF)/6-311+G<sup>\*\*</sup> and were visualized with MacMolPlt<sup>35</sup> and rendered using POV-RAY.<sup>36</sup>

Excited state calculations were performed using EE and SF variants of the EOM-CCSD and active space EOM-CC(2,3) methods.<sup>11</sup> EOM-SF calculations are based on the unrestricted

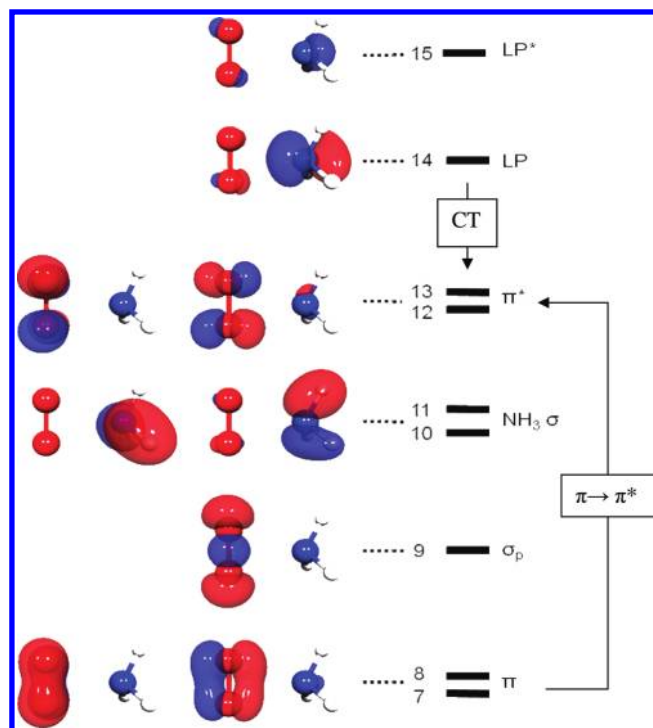


**Figure 2.** Molecular orbitals of the ammonia–oxygen complex with  $C_s$  symmetry. The symmetry plane is formed by the nitrogen and oxygen atoms.

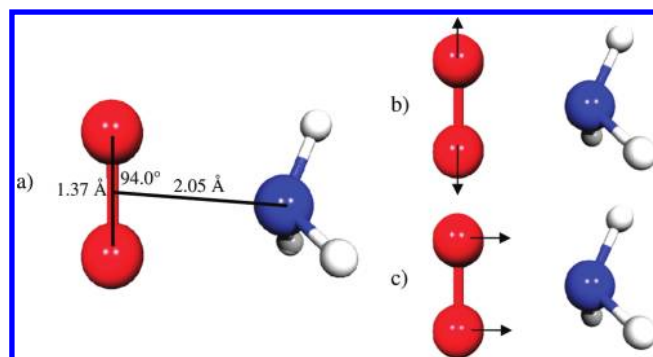


**Figure 3.** (a) Optimized EOM-SF-CCSD/6-311G<sup>\*</sup> geometry of the lowest triplet A'' CT state.  $\text{NH}_3\text{--O}_2$  degrees of freedom relevant for the geometry changes in the CT states: (b) oxygen bond length; (c) moiety separation. The geometry of the ammonia pyramid was held fixed during the geometry optimization.

HF triplet reference that consists of the closed-shell singlet on the ammonia and the  $^3\Sigma$  triplet on the oxygen. This state is the ground state of the  $\text{NH}_3\text{--O}_2$  complex. EOM-EE calculations employ restricted HF singlet reference corresponding to the closed-shell singlet on the ammonia and the closed-shell component of the oxygen  $^1\Delta$  state. The 6-311G<sup>\*</sup> basis set was used throughout. The ammonia lone pair (LP) orbital (orbital 14 in Figure 2) and the oxygen  $\pi$  and  $\pi^*$  orbitals (orbitals 7, 8, 12, and 13) are included in the active space in EOM-CC(2,3) calculations.

Potential energy slices along the ammonia–oxygen separation and the oxygen-bond-length coordinate (Figure 3b,c) were created for the low lying excited states using the EOM-CC methodologies outlined above. The  $\text{NH}_3\text{--O}_2$  separation was scanned from 1.8 to 3.6 Å in 0.2 Å increments with the oxygen

bond length fixed at 1.2 Å. Then, the oxygen bond length was scanned from 1.00 to 1.60 Å in 0.04 Å increments with the NH<sub>3</sub>–O<sub>2</sub> separation fixed at 2.4 Å.

Using a starting guess geometry based on the oxygen bond and moiety separation curves, the lowest A'' symmetry CT state was optimized using EOM-SF-CCSD/6-311G\*. The geometry of the ammonia pyramid was fixed during the optimization because a large scale geometry change in the amine would be unphysical in the tertiary amine systems of the experiments. Transition dipole moments and oscillator strengths were calculated at the optimized CT geometry using EOM-SF-CCSD/6-311G\* and EOM-EE-CCSD/6-311G\* levels of theory. Active space EOM-SF-CC(2,3)/6-311G\* and EOM-EE-CC(2,3)/6-311G\* excited state energy calculations were also performed at the optimized geometry of the lowest CT state.

## RESULTS AND DISCUSSION

The ground state optimizations of the ammonia–oxygen system resulted in the C<sub>s</sub> symmetry structure with the C<sub>3</sub> axis of the ammonia being nearly perpendicular (89.4°) to the O<sub>2</sub> bond axis and a 3.6 Å separation between the nitrogen atom and the oxygen molecule's center of mass. The geometries of the ammonia and oxygen molecules are essentially unchanged from their normal gas phase geometries. Similarly, Juranic et al.,<sup>5</sup> using semiempirical methods, discovered that equilibrium geometries have moiety separations between 3 and 4 Å. Essentially, in the ground state, the complex is only bound by long-range interactions and is unlikely to form a stable complex in solution.

The molecular orbitals for the ammonia–oxygen system are remarkably similar to the orbitals for individual ammonia and oxygen molecules (see Figure 2), though some mixing, particularly between the A' oxygen π and π\* orbitals and the ammonia A' orbitals, was observed at shorter NH<sub>3</sub>–O<sub>2</sub> separations. The electronic states in the complex can be characterized by either excitations on ammonia or oxygen moiety, or charge transfer excitations in which the electron density is shifted between the monomers. It is expected that the excitations within a monomer do not depend significantly on the intermonomer separation. The lowest energy state for the complex is composed of the closed-shell ammonia and oxygen in the triplet ground state. The three lowest excited states are dominated by redistribution of electrons on π\* orbitals of O<sub>2</sub> (orbitals 12 and 13) and correspond to <sup>1</sup>Δ<sub>g</sub> and <sup>1</sup>Σ<sub>g</sub><sup>+</sup> oxygen states. Oxygen π → π\* excitations and excitations on ammonia have high transition energies of ~6.5 eV. Excitations from a lone pair (LP) on NH<sub>3</sub> (orbital 14) to either of the π\* orbitals of O<sub>2</sub> result in CT states. Four electronic states (two singlets and two triplets) can originate from these excitations. The CT states are stabilized at shorter intermonomer separations. Indeed, all four of them are bound and have a minimum near 2.0 Å NH<sub>3</sub>–O<sub>2</sub> separations.

Remarkably, it is not easy to describe the CT states in a balanced way by EOM techniques. Figure 4 summarizes important determinants involved in the CT states and their description by EE and SF EOM methods. Using EOM-EE with the singlet closed-shell reference (corresponding to the <sup>1</sup>Δ state of O<sub>2</sub>), the pair of the A'' CT states is described by means of single excitations. However, the A' pair consists of formally doubly excited determinants with respect to the reference singlet state. As a result, the energy splitting between A' and A'' pairs is not correctly described by EOM-EE. The excitation energies of the A' CT states are significantly overestimated by EOM-EE.

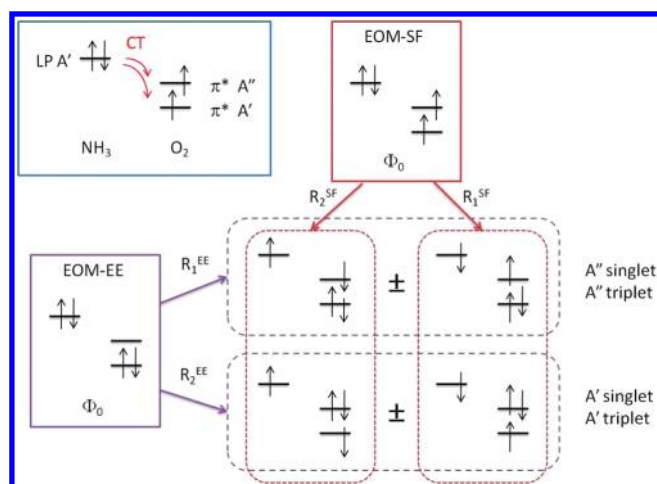


**Figure 4.** Description of CT states in NH<sub>3</sub>–O<sub>2</sub> complex by EOM-EE and EOM-SF. Lone pair (LP) orbital of NH<sub>3</sub> and two π\* orbitals of O<sub>2</sub> are shown (upper left panel). Four  $M_s = 0$  determinants with CT character (i.e., determinants obtained by excitation of an electron from NH<sub>3</sub> LP to π\* in O<sub>2</sub>) can be combined in two singlet and two triplet states. EOM-SF approach employing the high-spin triplet reference describes two of the CT determinants as singly excited ( $R_1^{SF}$ ) and two other determinants as doubly excited ( $R_2^{SF}$ ). As a result, all four CT states are described in a somewhat unbalanced way. In particular, the unbalanced description of the states is manifested in strong spin contamination. In the EOM-EE variant, A'' determinants are singly excited and A' determinants are doubly excited. Thus, the A'' singlet and triplet states are the singly excited states and are accurately described by EOM-EE. However, A' singlet and triplet are the doubly excited states and are not correlated in EOM-EE-CCSD. Therefore, excitation energies of A' states and energy splitting between A' and A'' pairs by EOM-EE-CCSD may have large errors.

Employing EOM-SF with the triplet reference (<sup>3</sup>Σ state of O<sub>2</sub>), one configuration of both A' and A'' states is obtained as a single excitation, while the other component is a double excitation with respect to the reference triplet. Unbalanced (mixed single–double) description of the states' components results in severe spin contamination as well as in inaccurate singlet–triplet energy differences. To improve the accuracy of description of these states, we employed the EOM-CC(2,3) method for both EE and SF variants, with the active space consisting of the three orbitals shown in Figure 4 (NH<sub>3</sub> LP and two O<sub>2</sub> π\*) as well as a pair of π orbitals on O<sub>2</sub>. Adding triple excitations decreases spin contamination and improves the accuracy of the excitation energies for problematic states, as discussed below.

Performance of the EOM-CCSD and EOM-CC(2,3) methods for low lying electronic states of NH<sub>3</sub>–O<sub>2</sub> is compared in Figure 5. As expected, EOM-EE-CCSD fails to describe the <sup>1</sup>Σ state of oxygen and overestimates its excitation energy by more than 3 eV (Figure 5a). This is because the leading configuration in the <sup>1</sup>Σ state is the closed-shell determinant that is doubly excited with respect to the EE reference determinant. As compared to EOM-EE-CC(2,3), EOM-EE-CCSD accurately describes two A'' CT states near their equilibrium at ~2 Å separation between NH<sub>3</sub> and O<sub>2</sub>. However, the accuracy becomes worse at longer NH<sub>3</sub>–O<sub>2</sub> separations, mainly because of mixing of the CT states with the π → π\* oxygen states, whose excitation energies are overestimated by EOM-EE-CCSD by more than 1.5 eV. Mixing of the CT states with the π → π\* states is a reason for including oxygen π orbitals in the active space in

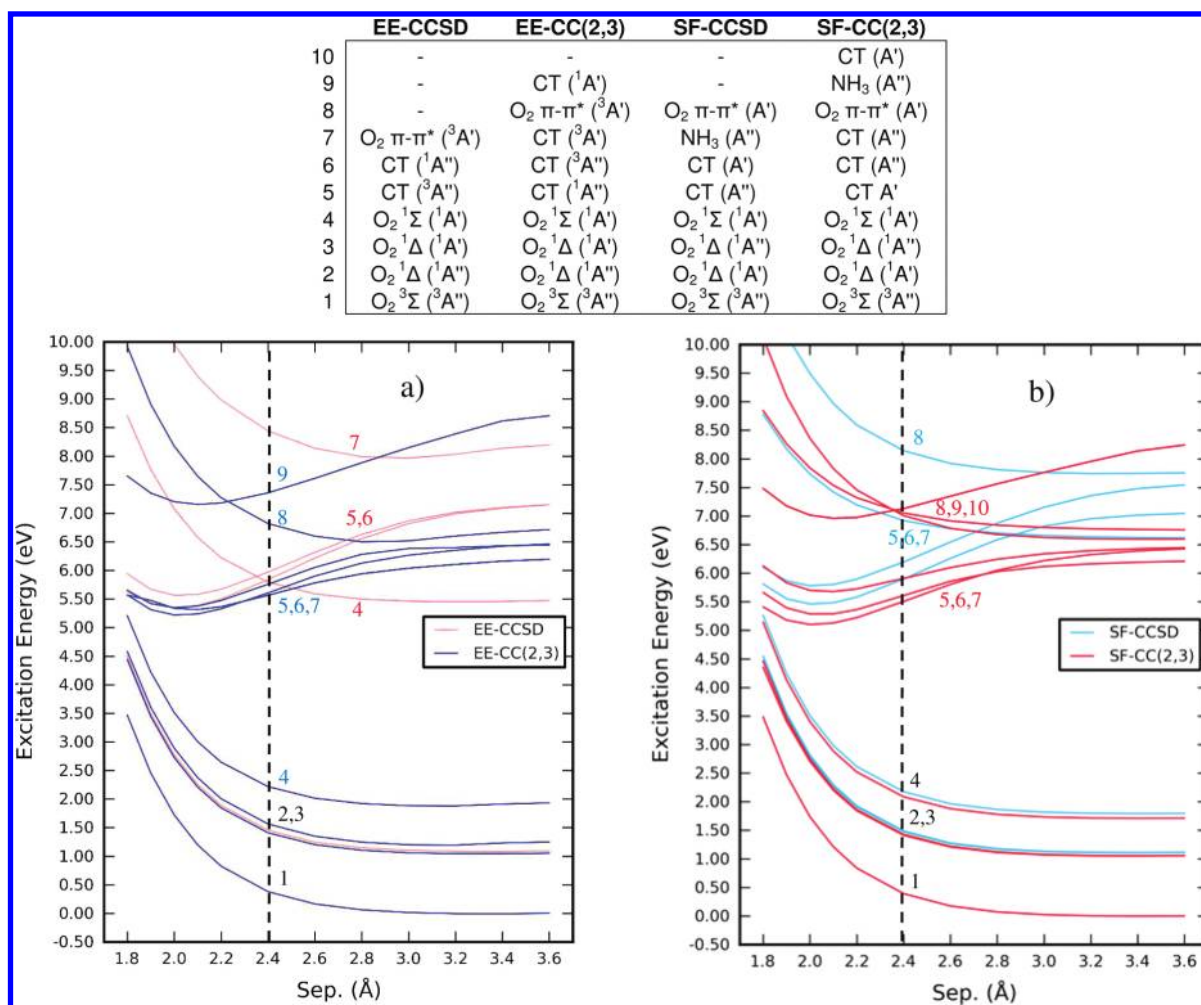


**Figure 5.** Comparison of EOM-CCSD and active space EOM-CC(2,3) excitation energies (in eV) along NH<sub>3</sub>–O<sub>2</sub> separation coordinate. (a) EE variant and (b) SF variant are shown. Zero energy for each method corresponds to the ground state equilibrium geometry.

EOM-CC(2,3). EOM-EE-CCSD fails to reproduce two A' CT states. As discussed above, these states are formally doubly excited in the EOM-EE formalism, and, similarly to the <sup>1</sup>Σ oxygen state, they are not correlated in EOM-EE-CCSD. As a result, their excitation energies are significantly overestimated by EOM-EE-CCSD. Additionally, being too high in energy, these states strongly interact with a rich manifold of higher lying oxygen and ammonia states (not shown in Figure 5), such that their unique assignment becomes problematic.

The SF variant of EOM-CCSD accurately describes diradical oxygen states (Figure 5b). However, it also significantly overestimates the excitation energy of the π → π\* oxygen state and two of the four CT states (not shown in Figure 5b). Description of two other CT states is reasonable around their equilibrium where they are low in energy and do not interact with other states. However, the accuracy deteriorates at large moiety separations because the CT states mix with the inaccurately described π → π\* states. Because of the unbalanced description of different components of the CT states by EOM-SF, these states are strongly spin contaminated. For example, the S<sup>2</sup> values for the states shown in Figure 5b are 1.04 and 1.13 in EOM-SF-CCSD (compared to 0.0 and 2.0 for spin-pure singlet and triplet states, respectively).

As was already discussed, the CT states prefer short inter-moiety separations. However, a transfer of an electron to the π\*

orbital of O<sub>2</sub> also destabilizes the O–O double bond. Indeed, the bonding character of the O–O bond becomes 1.5. This electron transfer leads to lengthening of the O–O bond in CT states. The potential energy curves along the oxygen bond coordinate are shown in Figure 6. Indeed, as clearly seen in Figure 6b, the CT states experience additional stabilization of ~1.4 eV upon lengthening of the O–O bond. In this respect, the CT states behave similarly to the π → π\* transition that also destabilizes the oxygen double bond. Based on the plot in Figure 6b, the optimal O–O distance for the CT states is 1.4 Å, which is ~0.2 Å longer than the equilibrium O–O bond length in O<sub>2</sub>.

Interestingly, the long-range behavior of the CT states along the monomer separation coordinate does not follow the 1/R asymptotic that is expected for the CT states. However, careful examination of the excitation amplitudes of the CT states shows that, with increasing separation, these states interact and mix with π → π\* oxygen states such that the CT character continuously transfers to higher lying states. In other words, the CT states experience avoided crossing with a manifold of π → π\* oxygen states (as well as some of the ammonia states). Effectively, the CT character at the moiety separations larger than 2.8–3.0 Å is spread over a large number of the electronic states. An additional consequence of interaction of the CT states with other higher lying states is a change in the energetic order of the CT states

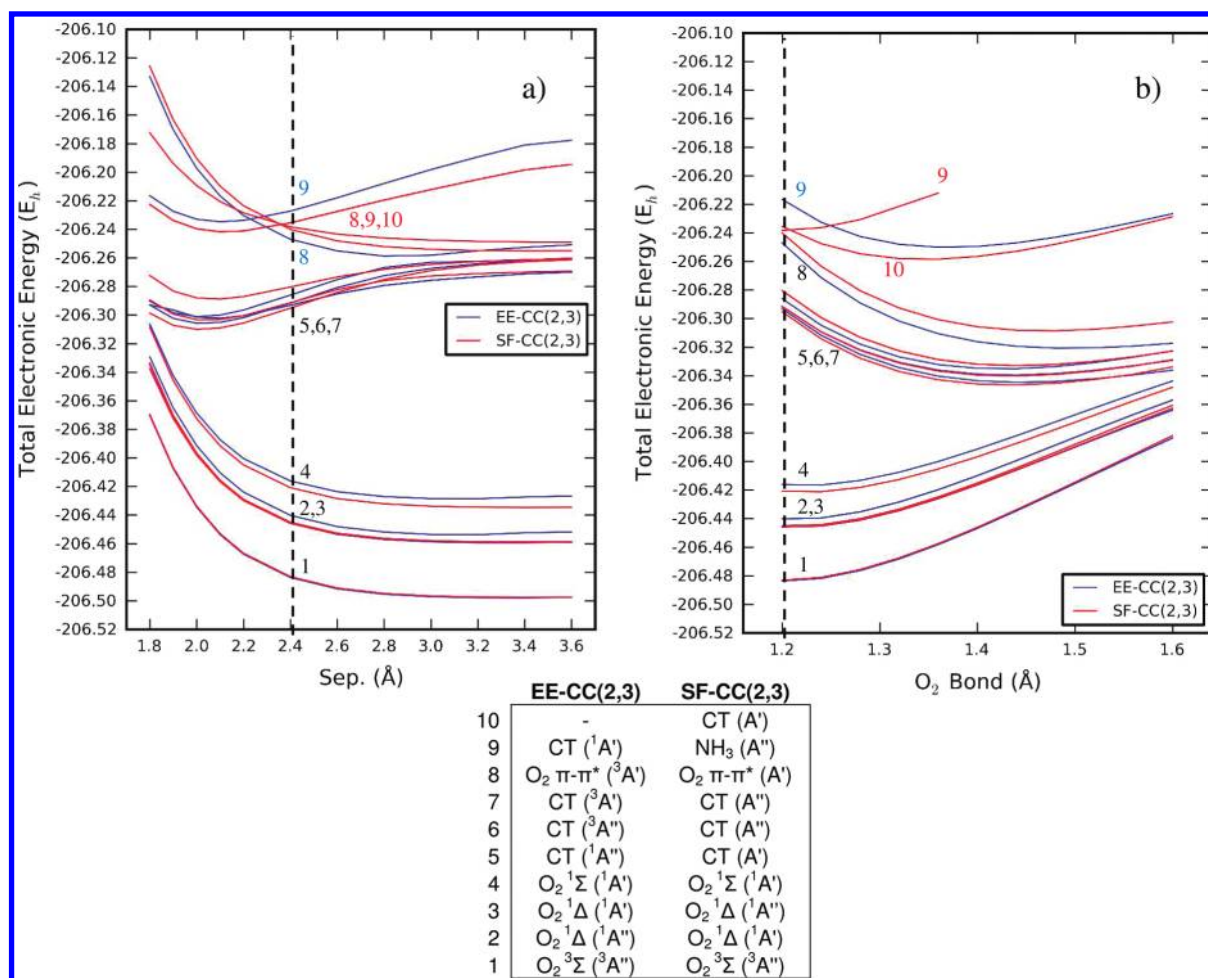


**Figure 6.** Active space EOM-SF-CC(2,3)/6-311G\* (red) and EOM-EE-CC(2,3)/6-311G\* (blue) potential energy curves (in hartrees) along (a) NH<sub>3</sub>-O<sub>2</sub> separation (with fixed O-O bond length of 1.2 Å) and (b) oxygen bond length (with fixed moiety separation of 2.4 Å). Five orbitals are included in the active space.

among themselves along the moiety separation coordinate. For example, the <sup>3</sup>A'' CT state by EOM-EE-CC(2,3) is the lowest at 1.8 Å separation but becomes second and even third at larger separations.

EOM-EE-CC(2,3) and EOM-SF-CC(2,3) methods agree with an overall picture of the electronic spectra of the NH<sub>3</sub>-O<sub>2</sub> complex (Figure 6). Thus, the triple excitations dramatically improve the description of this system and repair most of the deficiencies observed at the EOM-CCSD level. The discrepancies between EOM-EE-CC(2,3) and EOM-SF-CC(2,3) do not exceed 0.5 eV and are within 0.1–0.2 eV for most cases. This is opposed to the discrepancies up to 3 eV occurring at the EOM-CCSD level.

Despite many deficiencies in the description of the electronic states by either EOM-SF-CCSD or EOM-EE-CCSD, the shape of the potential energy curves of the lowest CT states near their equilibrium region is accurately reproduced. Therefore, we employ EOM-SF-CCSD for geometry optimization of the triplet A'' CT state (the geometry of ammonia was kept frozen in these calculations). The optimized geometry of the <sup>3</sup>A'' CT state (Figure 3) agrees with the expectations derived from the calculated potential energy curves; i.e., it possesses a short moiety separation and an elongated O-O bond. The most important difference is the ~4° angle between the ammonia C<sub>3</sub> axis and the

oxygen bond axis. The optimized geometry is used for calculating vertical and adiabatic excitation energies discussed in the next paragraph.

The fluorescence in tertiary amine dendrimers is observed around 460 nm with an absorbance maximum near 365 nm. The model considered in this work can provide only a qualitative understanding of electronic processes occurring in dendrimers since solvent and confinement effects as well as a more complicated structure of amine are not considered. For the NH<sub>3</sub>-O<sub>2</sub> system, the vertical excitation energies (Table 1) from the ground state to the lowest triplet CT states (that are mixed with π → π\* states at this region) are within the range 200–170 nm, which is too high in energy to be relevant to the PAMAM dendrimer experiments. However, the flat potential energy surface of the ground state suggests that significantly shorter intermonomer separations could be transiently accessible at room temperature. Furthermore, the presence of solvent is expected to stabilize CT states and lower the CT excitation energy. Also, it is possible in the confined space of the dendrimers for the oxygen molecules to be closer to the tertiary amines, further reducing the energy required to access the CT states. Vertical transitions from the optimized <sup>3</sup>A'' CT state to the ground state are 522.6 and 557.7 nm as predicted by EOM-EE-CC(2,3) and EOM-SF-CC(2,3). The oscillator strengths of

**Table 1. Adiabatic Excitation Energies and Vertical Excitation Energies at the Ground State (GS) and Optimized Charge Transfer State (CT) Geometries (in eV and nm) of the Triplet CT State ( $^3A''$ ) Calculated with EOM-EE and EOM-SF Methods in the 6-311G\*\* Basis Set<sup>a</sup>**

	EOM-EE-CC(2,3)		EOM-SF-CCSD		EOM-SF-CC(2,3)	
	eV	nm	eV	nm	eV	nm
vertical (GS)	6.91	179.7	7.07	175.4	6.23	199.3
vertical (CT)	2.37	552.6	2.62	473.1	2.23	557.5
adiabatic	4.06	305.7	4.35	285.4	3.89	318.9

<sup>a</sup> Observed fluorescence in tertiary amine dendrimers occurs around 460 nm with an absorbance maximum near 365 nm.

these transitions were estimated to be 0.0060 and 0.0073 at the EOM-EE-CCSD and EOM-SF-CCSD levels, respectively. The oscillator strengths are expected to increase in the condensed phase since solvation can mediate CT transitions. The excitation wavelengths predicted by EOM-CC(2,3) are 50–100 nm longer than the fluorescence emission from experimental work, suggesting that the lifetime of the CT state is smaller than the time required for the relaxation of the CT state to its minimum, and the fluorescence occurs from a nonequilibrium CT geometry. Alternatively, one could speculate about a possible involvement of the singlet states of oxygen in the observed luminescence. However, this would imply either absorption from the singlet oxygen state (that is limited by the amount of the singlet oxygen present in a system) or triplet-to-singlet internal conversion within a manifold of the CT states, and then emission from the singlet CT state. However, before exploring these pathways, the effects of the solvent and confinement should be characterized. This can be done by employing hybrid QM/MM (quantum mechanics/molecular mechanics) techniques developed by one of the authors.<sup>37,38</sup> These issues will be the topics of future work.

## CONCLUSIONS

The electronic structure of the ammonia–oxygen model system is investigated by the EOM-CC methods in order to explore origins of the blue-green luminescence observed in amine-containing dendrimers. The ammonia–oxygen complex in the ground state is bound by weak long-range interactions and is unlikely to form in solution. However, EOM-CC calculations reveal a manifold of four bound CT states, consistent with the hypothesis that the luminescence occurs due to the formation of the  $\text{NH}_3\text{--O}_2$  exciplex. The vertical excitation from the ground state to the lowest CT state is predicted to be  $\sim 170\text{--}200$  nm (vs  $\sim 365$  nm experimental). However, consistent with an essentially unbound ground state, the potential is relatively flat over a broad range of bond lengths. The population of species with bond lengths shorter than the weak minimum at  $3.6 \text{ \AA}$  will be described by a Boltzmann distribution and could be significant, particularly if excitation results in a bound excited state. In addition, solvent effects are expected to lower the CT excitation energy. The vertical excitation from the CT state is predicted to be  $\sim 520\text{--}560$  nm (vs 460 nm experimental), possibly indicating that the lifetime of the CT state is short compared to the time required for geometry relaxation. Ultimately, solvent, confinement, and amine structure effects will have to be considered before more quantitative and rigorous comparisons with experiment can be performed.

Inclusion of triple excitations in the EOM-CC formalism is necessary for describing excited states of amine–oxygen complexes since several states including the CT states have mixed or double excitation character in both the EE and SF variants. With inclusion of the triple excitations, discrepancies between the EE and SF variants of EOM-CC(2,3) are generally within 0.1–0.2 eV, which suggests that both methods provide accurate and realistic descriptions of the electronic spectrum of the ammonia–oxygen complex.

## AUTHOR INFORMATION

### Corresponding Author

\*Telephone: (765) 494-5255. E-mail: lslipchenko@purdue.edu.

## ACKNOWLEDGMENT

L.V.S. acknowledges support from NSF Career Grant CHE-0955419, ACS PRF Grant 49271-DNI6, and Purdue University. L.M.H. and G.J.S. acknowledge support from the Center for Direct Catalytic Conversion of Biomass to Biofuels (C3Bio), an Energy Frontier Research Center funded by the U.S. Department of Energy, Office of Science, Office of Basic Energy Sciences, Award No. DE-SC0000997.

## REFERENCES

- Wang, D.; Imae, T.; Miki, M. *J. Colloid Interface Sci.* **2007**, *306*, 222.
- Lee, W. I.; Bae, Y.; Bard, A. J. *J. Am. Chem. Soc.* **2004**, *126*, 8358.
- Yemul, O.; Imae, T. *Colloid Polym. Sci.* **2008**, *286*, 747.
- Chu, C.-C.; Imae, T. *Macromol. Rapid Commun.* **2009**, *30*, 89.
- Juranic, I.; Rzepa, H. S.; Yi, M. Y. *J. Chem. Soc., Perkin Trans. 2* **1990**, 877.
- Sekino, H.; Bartlett, R. J. *Int. J. Quantum Chem.* **1984**, *18*, 255.
- Koch, H.; Jensen, H. J. A.; Jorgensen, P.; Helgaker, T. *J. Chem. Phys.* **1990**, *93*, 3345.
- Stanton, J. F.; Bartlett, R. J. *J. Chem. Phys.* **1993**, *98*, 7029.
- Purvis, G. D. *J. Chem. Phys.* **1982**, *76*, 1910.
- Hirata, S.; Nooijen, M.; Bartlett, R. J. *Chem. Phys. Lett.* **2000**, *328*, 459.
- Slipchenko, L. V.; Krylov, A. I. *J. Chem. Phys.* **2005**, *123*, 084107.
- Bartlett, R. J. *Int. J. Mol. Sci.* **2002**, *3*, 579.
- Krylov, A. I. *Annu. Rev. Phys. Chem.* **2008**, *59*, 433.
- Levchenko, S. V.; Krylov, A. I. *J. Chem. Phys.* **2004**, *120*, 175.
- Krylov, A. I. *Acc. Chem. Res.* **2006**, *39*, 83.
- Slipchenko, L. V.; Krylov, A. I. *J. Chem. Phys.* **2002**, *117*, 4694.
- Slipchenko, L. V.; Krylov, A. I. *J. Chem. Phys.* **2003**, *118*, 6874.
- Slipchenko, L. V.; Krylov, A. I. *J. Phys. Chem. A* **2006**, *110*, 291.
- Stanton, J. F.; Gauss, J. J. *J. Chem. Phys.* **1999**, *111*, 8785.
- Sinha, D.; Mukhopadhyay, S.; Mukherjee, D. *Chem. Phys. Lett.* **1986**, *129*, 369.
- Stanton, J. F.; Gauss, J. J. *J. Chem. Phys.* **1994**, *101*, 8938.
- Nooijen, M.; Bartlett, R. J. *J. Chem. Phys.* **1995**, *102*, 3629.
- Wladyslawski, M.; Nooijen, M. In *Low-Lying Potential Energy Surfaces*; ACS Symposium Series 828; American Chemical Society: Washington, DC, 2002; p 65.
- Sattelmeyer, K. W.; Schaefer, H. F., III; Stanton, J. F. *Chem. Phys. Lett.* **2003**, *378*, 42.
- Shao, Y.; Molnar, L. F.; Jung, Y.; Kussmann, J.; Ochsenfeld, C.; Brown, S. T.; Gilbert, A. T. B.; Slipchenko, L. V.; Levchenko, S. V.; O'Neill, D. P.; DiStasio, R. A.; Lochan, R. C.; Wang, T.; Beran, G. J. O.; Besley, N. A.; Herbert, J. M.; Lin, C. Y.; Van Voorhis, T.; Chien, S. H.; Sodt, A.; Steele, R. P.; Rassolov, V. A.; Maslen, P. E.; Korambath, P. P.; Adamson, R. D.; Austin, B.; Baker, J.; Byrd, E. F. C.; Dachselt, H.; Doerksen, R. J.; Dreuw, A.; Dunietz, B. D.; Dutoi, A. D.; Furlani, T. R.;

Gwaltney, S. R.; Heyden, A.; Hirata, S.; Hsu, C. P.; Kedziora, G.; Khalliulin, R. Z.; Klunzinger, P.; Lee, A. M.; Lee, M. S.; Liang, W.; Lotan, I.; Nair, N.; Peters, B.; Proynov, E. I.; Pieniazek, P. A.; Rhee, Y. M.; Ritchie, J.; Rosta, E.; Sherrill, C. D.; Simmonett, A. C.; Subotnik, J. E.; Woodcock, H. L.; Zhang, W.; Bell, A. T.; Chakraborty, A. K.; Chipman, D. M.; Keil, F. J.; Warshel, A.; Hehre, W. J.; Schaefer, H. F.; Kong, J.; Krylov, A. I.; Gill, P. M. W.; Head-Gordon, M. *Phys. Chem. Chem. Phys.* **2006**, *8*, 3172.

(26) Becke, A. D. *J. Chem. Phys.* **1993**, *98*, 1372.

(27) Kohn, W.; Sham, L. J. *Phys. Rev.* **1965**, *140*, A1133.

(28) Becke, A. D. *Phys. Rev. A* **1988**, *38*, 3098.

(29) Hehre, W. J.; Ditchfield, R.; Pople, J. A. *J. Chem. Phys.* **1972**, *56*, 2257.

(30) Hariharan, P. C.; Pople, J. A. *Theor. Chim. Acta* **1973**, *28*, 213.

(31) Krishnan, R.; Binkley, J. S.; Seeger, R.; Pople, J. A. *J. Chem. Phys.* **1980**, *72*, 650.

(32) Clark, T.; Chandrasekhar, J.; Spitznagel, G. W.; Schleyer, P. V. *J. Comput. Chem.* **1983**, *4*, 294.

(33) Schmidt, M. W.; Baldridge, K. K.; Boatz, J. A.; Elbert, S. T.; Gordon, M. S.; Jensen, J. H.; Koseki, S.; Matsunaga, N.; Nguyen, K. A.; Su, S. J.; Windus, T. L.; Dupuis, M.; Montgomery, J. A. *J. Comput. Chem.* **1993**, *14*, 1347.

(34) Gordon, M. S.; Schmidt, M. W. In *Theory and Applications of Computational Chemistry*; Dykstra, C. E., Frenking, G., Kim, K. S., Scuseria, G. E., Eds.; Elsevier: New York, 2005; Chapter 41.

(35) Bode, B. M.; Gordon, M. S. *J. Mol. Graphics Modell.* **1998**, *16*, 133.

(36) Persistence of Vision Pty. Ltd., Williamstown, Victoria, Australia, 2004.

(37) Kosenkov, D.; Slipchenko, L. V. *J. Phys. Chem. A* **2010**, *115*, 392.

(38) Slipchenko, L. V. *J. Phys. Chem. A* **2010**, *114*, 8824.